

Preparation and Properties of Dimethyltetrafluorophosphate[†]

Christian Hohenstein and Andreas Kornath*

Department of Chemistry, Ludwig-Maximilians-University, Butenandtstrasse 5-13, 81377 Munich, Germany

Frank Neumann[‡]

Department of Chemistry, Technical University of Dortmund, Otto-Hahn-Strasse 6, D-44221 Dortmund, Germany. [‡]Current address: Innovation GmbH, Alexander Strasse 15, 44137 Dortmund, Germany.

Ralf Ludwig

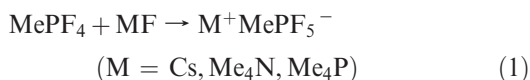
Department of Physical Chemistry, University of Rostock, Dr.-Lorenz-Weg 1, 18051 Rostock, Germany and Leibniz Institute for Catalysis at the University of Rostock, Albert-Einstein Strasse 29a, 18059 Rostock, Germany

Received December 8, 2009

Dimethyltrifluorophosphorane reacts with strong fluoride donors, such as CsF, Me₄NF, and Me₄PF, under formation of dimethyltetrafluorophosphates. The salts were characterized by infrared and Raman spectroscopy and in acetonitrile solutions by NMR spectroscopy. The experimental results show that only the *trans* isomer is formed. Theoretical calculations (B3LYP/6-31+G* and RHF/6-31+G*) of the *trans* and *cis* isomer yielded a difference of the Gibbs free energy of 29.4 kJ/mol (B3LPY/6-31+G*). The Me₄N⁺[Me₂PF₄][−] crystallizes in the orthorhombic space group *Pnma* with four formula units per unit cell and dimensions of *a* = 1303.5(3), *b* = 799.8(2), and *c* = 1023.8(4) pm. The phosphorus atom has an octahedral environment with P–C distances of 183.4(3) pm and P–F bond lengths in the range between 166.1(1) and 168.2(1) pm. In the crystal packing, anions and cations are linked via weak fluorine hydrogen contacts forming a three-dimensional network.

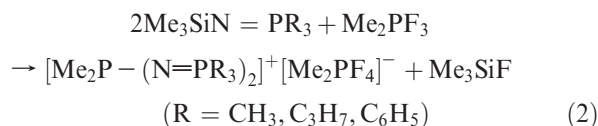
Introduction

The Lewis acid–base properties of methylfluorophosphoranes Me_nPF_{5−n} (*n* = 1–4) obviously display a dramatic change within the series. MePF₄ has typical properties of a Lewis acid, whereas the last member, Me₄PF, serves as a source for “naked” fluoride.^{1,2} Methyltetrafluorophosphorane reacts easily with alkali metal fluorides or Me₄NF under formation of methylpentafluorophosphates (eq 1).¹



In contrast to the well characterized MePF₅[−]-anion,¹ the homologous dimethyltetrafluorophosphate was described

only as a product of the reaction of dimethyltrifluorophosphorane with *N*-trimethylsilylphosphine imines (eq 2).^{3–6}



In all cases the anion was identified only by nuclear magnetic resonance (NMR) spectra, which shows the exclusive formation of the *trans* isomer of dimethyltetrafluorophosphate. The preparation by CsF and dimethyltrifluorophosphorane or by aminolysis of Me₂PF₃ was negated by Schmutzler et al., and the authors assumed that the anion can be only stabilized

[†] Dedicated to Prof. Dr. Bernhard Lippert on the occasion of his 65th birthday.
*E-mail: andreas.kornath@cup.uni-muenchen.de.

(1) Kornath, A.; Neumann, F.; Ludwig, R. *Z. Anorg. Allg. Chem.* **2003**, *629*, 615.

(2) Kornath, A.; Neumann, F.; Oberhammer, H. *Inorg. Chem.* **2003**, *42*, 2894.

(3) Stadelmann, W.; Stelzer, O.; Schmutzler, R. *J. Chem. Soc. D* **1971**, *22*, 1456.

(4) Stadelmann, W.; Stelzer, O.; Schmutzler, R. *Z. Anorg. Allg. Chem.* **1971**, *385*, 142.

(5) Stadelmann, W. *Gov. Rep. Announce. Index (U.S.)* **1982**, *82*, 272.

(6) Bartsch, R.; Harris, R. K.; Norval, E. M.; Stadelmann, W.; Stelzer, O.; Schmutzler, R. *Phosphorous Sulfur Silicon Relat. Elem.* **1988**, *40*, 135.

by the larger counterion ($[\text{Me}_2\text{P}-(\text{N}=\text{PR}_3)_2]^+$).^{3,7} This implicates a low Lewis acidity of Me_2PF_3 , thus it might only react with a more powerful fluoride ion donor and, therefore, serve as a useful probe for reactivity studies on various sources for “naked” fluoride. In this context, we would like to present the preparation and properties of dimethyltetrafluorophosphates.

Experimental Section

Apparatus and Materials. All synthetic work and sample handling were performed employing standard Schlenk techniques and a standard vacuum line (stainless steel or glass, respectively). Organic solvents and alkali metal fluorides were dried by standard methods. The synthesis of Me_4NF and Me_4PF was carried out by known literature methods.^{2,8} Dimethyltrifluorophosphorane was prepared by the reaction of $(\text{Me}_2\text{P}(\text{S})-\text{P}(\text{S})\text{Me}_2$ with SbF_3 .^{9,10}

Caution! The toxicities of dimethyltrifluorophosphorane and dimethyltetrafluorophosphates are not known. Hydrolysis with alcohols should be avoided, because of a potential formation of extremely toxic fluorophosphorous esters!

Infrared spectra were recorded on a Bruker IFS 113v spectrophotometer. Spectra of dry powders were obtained using a CsBr plate coated with the neat sample. The Raman spectra were recorded on an ISA T64000 spectrometer using an Ar^+ laser tube (514.5 nm) from Spectra Physics. The spectra were recorded in a glass cell. The NMR spectra were recorded with a Bruker DBX 300 spectrometer. Both 85% H_3PO_4 and F11 were used as standards. Single crystals were placed in Lindemann capillaries in a cooled stream of dry nitrogen, and the X-ray diffraction studies were carried out using an ENRAF Nonius Cappa CCD diffractometer.

Synthesis of $\text{Na}[\text{Me}_2\text{PF}_4]$. Dry NaF (0.63 g; 15 mmol) was placed into a 25 mL glass vessel with a grease-free valve, and 2.5 g acetonitrile and 2.12 g (18 mmol) Me_2PF_3 were condensed at -196°C . The frozen mixture was warmed to room temperature and kept for 12 h in an ultrasonic bath. The solvent and excess of Me_2PF_3 were removed in dynamic vacuum at -15°C . The weight of the residual colorless solid (1.74 g) indicates a content of 63% of formed $\text{Na}[\text{Me}_2\text{PF}_4]$. The salt decomposes in a dynamic vacuum at room temperature or at 107°C in an inert atmosphere of 1013 hPa, respectively.

Synthesis of $\text{K}[\text{Me}_2\text{PF}_4]$. Dry KF (0.99 g; 17 mmol) was placed into a 25 mL glass vessel with a grease-free valve. After condensation of 2.5 g acetonitrile and 2.36 g (20 mmol) Me_2PF_3 at -196°C , the mixture was warmed to room temperature and kept for 12 h in an ultrasonic bath. The volatiles were removed in dynamic vacuum at -5°C . The weight of the colorless residual (2.63 g) represents a yield of 82% besides remaining KF. The salt decomposes slowly in a dynamic vacuum at room temperature or at 130°C in an inert atmosphere of 1013 hPa, respectively.

Synthesis of $\text{Cs}[\text{Me}_2\text{PF}_4]$. In a 25 mL glass vessel with a grease-free valve 1.51 g (10 mmol) dried CsF was placed, and 2.5 g acetonitrile and 1.42 g (12 mmol) Me_2PF_3 were condensed at -196°C . After warming to room temperature, the mixture was kept for 12 h in an ultrasonic bath. The volatiles were removed in dynamic vacuum at room temperature. The yield of colorless $\text{Cs}[\text{Me}_2\text{PF}_4]$ was 96%. The salt decomposes at ca. 160°C in an inert atmosphere.

Synthesis of $\text{Me}_4\text{N}[\text{Me}_2\text{PF}_4]$. In a 25 mL glass vessel with a grease-free valve, 0.2 g (2 mmol) of well dried Me_4NF was

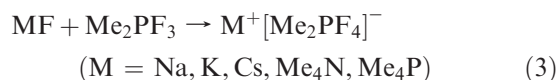
placed, and 3 g acetonitrile and 0.37 g (3 mmol) Me_2PF_3 were condensed at -196°C . The mixture was warmed to room temperature and stirred for 1 h. The volatiles were removed in dynamic vacuum. The colorless microcrystalline $\text{Me}_4\text{N}[\text{Me}_2\text{PF}_4]$ was formed in quantitative yield. It decomposes at ca. 140°C . The growing of suitable crystals for X-ray diffraction studies was achieved by slow removal of acetonitrile from a saturated solution of $\text{Me}_4\text{N}[\text{Me}_2\text{PF}_4]$ over four days. The single crystals for X-ray studies were measured by Raman spectroscopy to ensure that they represent the whole sample of the solid. Raman spectral data for $\text{Me}_4\text{N}[\text{Me}_2\text{PF}_4]$ [cm^{-1} (relative intensity)]: 378 (4), 388 (3), 411 (2), 463 (5), 480 (7), 517 (6), 598 (2), 640 (18), 655 (5), 701 (2), 743 (6), 759 (31), 950 (9), 956 (14), 1176 (2), 1183 (1), 1288 (2), 1413 (3), 1420 (2), 1468 (18), 1483 (6), 1487 (5), 1500 (2), 1558 (1), 2812 (6), 2824 (6), 2860 (14), 2937 (66), 2938 (40), 2966 (73), 2994 (76), 3043 (100). IR spectral data for $\text{Me}_4\text{N}^+[\text{Me}_2\text{PF}_4]^-$ [cm^{-1}]: 282 m, 338 m, 403 w, 455 m, 478 w, 529 w, 710 w, 729 w, 757 vw, 892 vw, 947 vs, 1050 vw br, 1231 s, 1403 m, 1487 s, 2449 vw, 2956 vw, 3017 w.

Synthesis of $\text{Me}_4\text{P}[\text{Me}_2\text{PF}_4]$. In a 25 mL glass vessel with a grease-free valve, 0.20 g (1.8 mmol) Me_4PF was placed, and 3 g acetonitrile and 0.31 g (2.6 mmol) Me_2PF_3 were condensed at -196°C . After warming to room temperature, the mixture was stirred for 1 h, and the volatiles were removed in dynamic vacuum. The colorless $\text{Me}_4\text{P}[\text{Me}_2\text{PF}_4]$ was formed in quantitative yield. The salt starts to decompose at ca. 110°C in an inert atmosphere. Raman spectral data for $\text{Me}_4\text{P}[\text{Me}_2\text{PF}_4]$ [cm^{-1} (relative intensity)]: 249 (11), 291 (11), 390 (2), 407 (2), 475 (8), 514 (4), 641 (6), 646 (11), 650 (18), 780 (9), 1424 (13), 2927 (61), 2937 (39), 3006 (100).

Computational Methods. The quantum chemical calculations of the *cis* and *trans* Me_2PF_4^- anions were performed at various levels of theory by using the Hartree–Fock method and the density functional theory (DFT) method B3LYP.^{11,12} As the basis set, we have chosen 6-31+G*. In earlier studies, we found by comparison of different theoretical methods for methylfluorophosphates, that RHF/6-31+G* and B3LYP/6-31+G* yield geometry parameters and vibrational frequencies that agree well with experimental data.^{1,2} The methods and the basis set were all implemented in the Gaussian 98 Program.¹³

Results and Discussion

Synthesis and Properties of $[\text{Me}_2\text{PF}_4]^-$ Salts. Me_2PF_3 reacts with the alkali metal fluorides NaF, KF, and CsF and with the tetramethylpnicoxonium fluorides Me_4PF and Me_4NF under formation of dimethyltetrafluorophosphates (eq 3). The colorless salts are stable at room temperature, hygroscopic and, as alkali metal salts, only slightly soluble in acetonitrile.



(11) Hehre, W. G.; Radom, L.; Schleyer, P. v.; Pople, J. A. *Ab initio Molecular Orbital Theory*; Wiley: New York, 1986.

(12) Becke, A. D. *J. Chem. Phys.* **1996**, *104*, 1040.

(13) Frisch, M. J.; Trucks, G. W.; Schlegel, H. B.; Scuseria, G. E.; Robb, M. A.; Cheeseman, J. R.; Zakrzewski, V. G.; Montgomery, J. A., Jr.; Stratmann, R. E.; Burant, J. C.; Dapprich, S.; Millam, J. M.; Daniels, A. D.; Kudin, K. N.; Strain, M. C.; Farkas, O.; Tomasi, J.; Barone, V.; Cossi, M.; Cammi, R.; Mennucci, B.; Pomelli, C.; Adamo, C.; Clifford, S.; Ochterski, J.; Petersson, G. A.; Ayala, P. Y.; Cui, Q.; Morokuma, K.; Malick, D. K.; Rabuck, A. D.; Raghavachari, K.; Foresman, J. B.; Cioslowski, J.; Ortiz, J. V.; Stefanov, B. B.; Liu, G.; Liashenko, A.; Piskorz, P.; Komaromi, I.; Gomperts, R.; Martin, R. L.; Fox, D. J.; Keith, T.; Al-Laham, M. A.; Peng, C. Y.; Nanayakkara, A.; Gonzalez, C.; Challacombe, M.; Gill, P. M. W.; Johnson, B. G.; Chen, W.; Wong, M. W.; Andres, J. L.; Head-Gordon, M.; Replogle, E. S.; Pople, J. A. *Gaussian 98*, revision A.1; Gaussian, Inc.: Pittsburgh, PA, 1998.

(7) Stadelmann, W.; Stelzer, O.; Schmutzler, R. *J. Chem. Soc. A* **1970**, *21*, 2364.

(8) Christe, K. O.; Wilson, W. W.; Wilson, R. D.; Bau, R.; Feng, J. *J. Am. Chem. Soc.* **1990**, *112*, 7619.

(9) Schmutzler, R. *Inorg. Synth.* **1967**, *9*, 63.

(10) Seel, F.; Rudolph, K. *Z. Anorg. Allg. Chem.* **1968**, *363*, 233.

The yields of the $[\text{Me}_2\text{PF}_4]^-$ salts resulting from the reaction of Me_2PF_3 with Me_4PF and Me_4NF , respectively, in the presence of acetonitrile were quantitative within one hour. The presence of acetonitrile ensures moderate reaction conditions, since the neat starting materials occasionally react vigorously. Alkali metal fluorides react slowly with neat Me_2PF_3 , and when an ultrasonic bath has been employed, the yields of the resulting $[\text{Me}_2\text{PF}_4]^-$ salts were below 30%. The content of $[\text{Me}_2\text{PF}_4]^-$ increases in the series of alkali metal salts from 63% for Na^+ to 96% for Cs^+ in the presence of acetonitrile as solvent. Similar observations have been made for alkali metal fluorides with moderate Lewis acids, such as SO_2 or MePF_4 .^{1,14}

The alkali metal salts decompose at 107 (Na^+), 130 (K^+), and 160 °C (Cs^+), respectively, under formation of the alkali metal fluorides and Me_2PF_3 . In case of Na^+ - $[\text{Me}_2\text{PF}_4]^-$, the loss of Me_2PF_3 was also observed at room temperature when a dynamic vacuum of ca. 1 hPa was employed. The thermal decomposition of $\text{Me}_4\text{N}^+[\text{Me}_2\text{PF}_4]^-$ (140 °C) and $\text{Me}_4\text{P}^+[\text{Me}_2\text{PF}_4]^-$ (110 °C) is more complex. Probably, the first step is a simple dissociation in Me_2PF_3 , and the fluorides followed by decomposition of the fluorides and subsequent reactions lead to yellow insoluble solids and various volatile products, which have not been identified.

In contrast to our findings, it has been previously reported that the $[\text{Me}_2\text{PF}_4]^-$ anion can only be stabilized by a large counterion, such as $[\text{Me}_2\text{P}-(\text{N}=\text{PR}_3)_2]^+$.^{3,7} Reactions of fluorides with Lewis acids can be described thermodynamically by eqs 4 and 5 derived from the Born–Haber cycle, ignoring small differences in heat capacity and polymorphic transitions between 0 and 298 K.¹⁴

$$\Delta H_{\text{f}}^\circ = \Delta H_{\text{F}}^\circ + \Delta U \quad (4)$$

$$\Delta G_{\text{f}}^\circ = \Delta H_{\text{F}}^\circ + \Delta U - T\Delta S^\circ \quad (5)$$

The heat of formation ($\Delta H_{\text{f}}^\circ$) is expressed as the sum of the fluoride ion affinity ($\Delta H_{\text{F}}^\circ$) and the change in lattice energy (ΔU). Christe et al. have demonstrated, on the basis of Born–Haber cycle calculations for a series of fluoride ion transfer reactions, that the change in lattice energy is in general considerably small (less than ca. 60 kJ mol^{-1}) for large counterions, such as $[\text{Me}_2\text{P}-(\text{N}=\text{PR}_3)_2]^+$ and that it increases with decreasing size of the counterion.¹⁵ Consequently, when a reaction only takes place with a fluoride of a large counterion, the fluoride affinity ($\Delta H_{\text{F}}^\circ$) of the Lewis acid should be small. The fluoride affinity of Me_2PF_3 is not known, and theoretical calculations of fluoride ion affinity are difficult because the electron affinity of fluorine atoms is hard to calculate.¹⁶ Compared with our previous studies on methylfluorophosphoranes,^{1,17} the Lewis acidity of Me_2PF_3 is lower than that of MePF_4 and comparable to that of MePF_3H . Overall, this is an expected trend in which

Table 1. Comparison of the NMR Data of *Trans*-Dimethyltetrafluorophosphate with Hydrido- and Methyl-Substituted Fluorophosphates

anion	^{31}P	^{19}F	^1H
$[\text{PF}_6]^-$	$\delta = -142.9 \text{ ppm}^a$ $^1J_{\text{PF}} = 706.5 \text{ Hz}$	$\delta_{\text{F}} = -70.9 \text{ ppm}^a$ $^1J_{\text{PF}} = 706.6 \text{ Hz}$	—
$[\text{HPF}_5]^-$	$\delta = -141.5 \text{ ppm}^b$ $^1J_{\text{PF}_e} = 820 \text{ Hz}$ $^1J_{\text{PF}_a} = 730 \text{ Hz}$ $^1J_{\text{PH}} = 945 \text{ Hz}$	$\delta_{\text{F}_e} = -56.0 \text{ ppm}^c$ $^1J_{\text{PF}_e} = 818 \text{ Hz}$ $^2J_{\text{HF}_e} = 126 \text{ Hz}$ $\delta_{\text{F}_a} = -65.9 \text{ ppm}$ $^1J_{\text{PF}_a} = 730 \text{ Hz}$ $^2J_{\text{HF}_a} \approx 0 \text{ Hz}$ $^2J_{\text{F}_a\text{F}_e} = 42 \text{ Hz}$	—
$[\text{H}_2\text{PF}_4]^-$	$\delta = -123.5 \text{ ppm}^d$	$\delta = -53.3 \text{ ppm}^e$ $^1J_{\text{PF}} = 806 \text{ Hz}$ $^2J_{\text{HF}} = 123 \text{ Hz}$	$\delta = 5.80 \text{ ppm}^e$ $^1J_{\text{PH}} = 936 \text{ Hz}$ $^2J_{\text{HF}} = 123 \text{ Hz}$
$[\text{MePF}_5]^-$	$\delta = -126.4 \text{ ppm}^f$ $^1J_{\text{PF}_e} = 829 \text{ Hz}$ $^1J_{\text{PF}_a} = 680 \text{ Hz}$	$\delta_{\text{F}_e} = -45.8 \text{ ppm}^f$ $\delta_{\text{F}_a} = -57.6 \text{ ppm}$ $^1J_{\text{PF}_e} = 829 \text{ Hz}$ $^1J_{\text{PF}_a} = 680 \text{ Hz}$ $^2J_{\text{F}_a\text{F}_e} = 41 \text{ Hz}$	$\delta = 1.05 \text{ ppm}^g$ $^2J_{\text{HP}} = 20 \text{ Hz}$ $^3J_{\text{HF}_e} = 9 \text{ Hz}$
$[\text{Me}_2\text{PF}_4]^-$ ^f	—	$\delta = -20.9 \text{ ppm}^g$ $^1J_{\text{PF}} = 856 \text{ Hz}$ $^3J_{\text{FH}} = 10 \text{ Hz}$	$\delta = 1.07 \text{ ppm}^g$ $^2J_{\text{HP}} = 20.5 \text{ Hz}$ $^3J_{\text{HF}} = 9.5 \text{ Hz}$
$[\text{Me}_2\text{PF}_4]^-$ (this work)	$\delta = -108.8 \text{ ppm}$ $^1J_{\text{PF}} = 854 \text{ Hz}$	$\delta = -21.2 \text{ ppm}$ $^1J_{\text{PF}} = 854 \text{ Hz}$ $^3J_{\text{FH}} \approx 10 \text{ Hz}$	$\delta = 1.00 \text{ ppm}$ $^2J_{\text{HP}} = 21.0 \text{ Hz}$ $^3J_{\text{HF}} = 9 \text{ Hz}$
$[\text{MePF}_4\text{H}]^-$	$\delta = -118.0 \text{ ppm}^h$ $^1J_{\text{PF}} = 826 \text{ Hz}$ $^1J_{\text{PH}} = 966 \text{ Hz}$ $^2J_{\text{PH}} = 18 \text{ Hz}$	$\delta = -35.0 \text{ ppm}^h$ $^1J_{\text{PF}} = 826 \text{ Hz}$ $^2J_{\text{FH}} = 133 \text{ Hz}$ $^3J_{\text{FH}} \approx 10 \text{ Hz}$	—

^a From ref 18. ^b $(\text{CH}_3\text{CH}_2)_3\text{NH}^+[\text{HPF}_5]^-$ from ref 19. ^c $\text{Me}_3\text{NH}^+[\text{HPF}_5]^-$ from ref 20. ^d $\text{K}^+[\text{H}_2\text{PF}_4]^-$ from ref 21. ^e $\text{Me}_3\text{NH}^+[\text{H}_2\text{PF}_4]^-$ from ref 19. ^f $[\text{CH}_3\text{PF}(\text{OCH}_2\text{CH}_2)_2\text{NH}]^+[\text{MePF}_5]^-$ from ref 22. ^g $[\text{Me}_2(\text{N}=\text{PMe}_2)]^+[\text{Me}_2\text{PF}_4]^-$ from ref 3. ^h $\text{Me}_4\text{N}^+[\text{MePF}_4\text{H}]^-$ from ref 17.

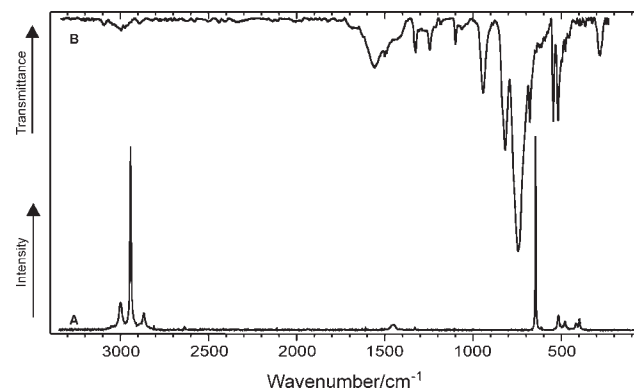


Figure 1. Raman spectrum (trace A) and infrared spectrum (trace B) of $\text{Cs}^+[\text{Me}_2\text{PF}_4]^-$.

PF_5 has the highest Lewis acidity, and substitution of a fluorine atom by a methyl group or a hydrogen atom leads to a decrease in Lewis acidity. The Lewis acid–base properties of Me_3PF_2 are not known yet, but the Me_4PF is already a strong fluoride donor (“naked” fluoride).

NMR Spectra. The NMR spectroscopic data of $\text{Me}_4\text{N}^+[\text{Me}_2\text{PF}_4]^-$ solved in acetonitrile are summarized in Table 1 together with data for hydrido- and methylfluoro phosphates.^{3,17–22} Similarly to the $[\text{MeHPF}_4]^-$ salts and accordingly

(14) Kornath, A.; Neumann, F.; Ludwig, R. *Inorg. Chem.* **1997**, *36*, 5570.

(15) Christe, K. O.; Brooke Jenkins, H. D. *J. Am. Chem. Soc.* **2003**, *125*, 9457.

(16) Christe, K. O.; Dixon, D. A.; McLemore, D.; Wilson, W. W.; Sheehy, J. A.; Boatz, J. A. *J. Fluorine Chem.* **2000**, *101*, 151.

(17) Kornath, A.; Neumann, F.; Ludwig, R. *Z. Anorg. Allg. Chem.* **2003**, *629*, 609.

(18) Raab, V.; Kipke, J.; Gschwind, R. M.; Sundermeyer, J. *Chem.—Eur. J.* **2002**, *8*, 1682.

(19) Riesel, L.; Kant, M. *Z. Chem.* **1984**, *10*, 382.

(20) Cowley, A. H.; Wisian, P. J.; Sanchez, M. *Inorg. Chem.* **1977**, *16*, 843.

(21) Minkwitz, R.; Liedtke, A. *Z. Naturforsch.* **1989**, *44b*, 679.

(22) Robert, D.; Gawad, H. A.; Riess, J. G. *Bull. Soc. Chim. Fr.* **1987**, *3*, 511.

Table 2. Experimental and Calculated Vibrational Frequencies (cm^{-1}) of *Trans*-Dimethyltetrafluorophosphate

	RHF/6-31+G** ^a		Cs ⁺ [Me ₂ PF ₄] ⁻		assignment
	IR-int.	Raman-act.	IR	Raman	
2986.6	99.7	68.3	3007 w		$\nu_{\text{as}}(\text{CH}_3)$ in phase
2986.1	8.2	69.0	2986 w	2999 (36)	$\nu_{\text{as}}(\text{CH}_3)$
2985.4	98.3	60.7			$\nu_{\text{as}}(\text{CH}_3)$ in phase
2984.1	1.9	83.8			$\nu_{\text{as}}(\text{CH}_3)$
2924.3	0.0	259.8		2942 (100)	$\nu_{\text{s}}(\text{CH}_3)$ in phase
2923.4	78.5	0.3	2906 vw		$\nu_{\text{s}}(\text{CH}_3)$
				2867 (23)	
			1567 w, br		$\nu_{\text{as}}(\text{PC}_2) + \nu_{\text{as}}(\text{PF}_2)$
1478.4	2.4	4.9	1506 vvw		$\delta_{\text{as}}(\text{CH}_3)$ in phase
1477.4	2.1	4.7	1494 vvw		$\delta_{\text{as}}(\text{CH}_3)$ in phase
1477.2	0.1	9.5		1451 (7)	$\delta_{\text{as}}(\text{CH}_3)$
1475.7	0.0	6.8			$\delta_{\text{as}}(\text{CH}_3)$
1353.9	38.6	0.0	1331 w		$\delta_{\text{s}}(\text{CH}_3)$
1353.5	0.3	8.0		1328 (0.4)	$\delta_{\text{s}}(\text{CH}_3)$ in phase
			1252 w		$\nu(\text{PF}_4)$ in phase + $\nu_{\text{as}}(\text{PF}_2)$
			1215 vw		$\nu(\text{PF}_4)$ out of phase + $\nu_{\text{as}}(\text{PF}_2)$
			1188 vw		
			1103 w		
			946 m		$\rho(\text{CH}_3)$ in phase
970.7	84.8	0.0			$\rho(\text{CH}_3)$ in phase
969.6	82.5	0.0			$\rho(\text{CH}_3)$
931.3	0.0	2.8			$\rho(\text{CH}_3)$
930.9	0.2	2.9			$\rho(\text{CH}_3)$
821.0	328.4	0.1	823 ms		$\nu_{\text{as}}(\text{PC})$
683.7	405.6	0.1	748 vs		$\nu_{\text{as}}(\text{PF})$
682.8	405.3	0.1			$\nu_{\text{as}}(\text{PF})$
			680 m		
626.5	0.0	26.4		644 (47)	$\nu_{\text{s}}(\text{PC})$
518.2	120.0	0.0	544 ms		$\delta(\text{PF}_4)$ umbrella
501.1	0.3	6.1	520 ms	512 (13)	$\nu(\text{PF})$ in phase
478.1	0.2	2.0	478 m	476 (6)	$\nu(\text{PF})$ out of phase
414.3	4.1	0.0		414 (4)	$\delta(\text{CPC}/\text{FPF})$
411.8	4.0	0.0			$\delta(\text{CPC}/\text{FPF})$
386.9	0.0	0.5		394 (5)	$\delta(\text{CPF})$ sciss
379.4	0.0	0.6			$\delta(\text{PF}_4)$ in plane
377.6	0.2	0.5	364 w		$\delta(\text{CPF})$ sciss
291.7	0.0	0.0			$\delta(\text{PF}_4)$ out of plane
257.1	0.6	0.0	282 m		$\delta(\text{CPC}/\text{FPF})$
239.9	0.7	0.1			$\delta(\text{CPC}/\text{FPF})$
50.8	0.0	0.3			$\tau(\text{CH}_3)$
1.4	0.2	0.0			$\tau(\text{CH}_3)$ in phase

^a Frequencies are scaled with an empirical factor 0.91; IR intensities in km/mol ; and Raman activities in $\text{\AA}^4/\text{u}$.

to previous studies of the $[\text{Me}_2\text{PF}_4]^-$ anion, the *trans* isomer is observed in solution exclusively. In accordance with a *trans* structure, the ^{19}F NMR spectrum displays a doublet ($^1J_{\text{PF}} = 854$ Hz) of doublets ($^3J_{\text{FH}} \cong 10$ Hz) at -21.2 ppm. The ^{31}P NMR spectrum shows at -108.8 ppm a quintet ($^1J_{\text{PF}} = 854$ Hz) with relatively broad signals indicating the expected further splitting into septets with an $^3J_{\text{PH}} = 21$ Hz, which was observed in the ^1H NMR spectrum. The ^{31}P chemical shift of the methylfluorophosphates displays a trend in which the formal substitution of one fluorine atom by one methyl group causes a shift toward the high field on the order of 17 ppm.

Vibrational Spectra. The infrared and Raman spectra of $\text{Cs}^+[\text{Me}_2\text{PF}_4]^-$ are shown in Figure 1 and summarized in Table 2. Theoretically calculated frequencies of the *trans* and *cis* isomer have been considered to compare and assign the vibrational modes (Table 3) and to ensure that the solid state consists of one isomer. For both isomers, the calculations, which are discussed later, predict a C_1 symmetry with 33 fundamental frequencies which should be all Raman and infrared active. The assignments of the vibrational modes were made by consideration of the Cartesian displacement coordinates.

For both calculated $[\text{Me}_2\text{PF}_4]^-$ isomers, the stretching and deformation modes of the methyl group occur in the typical regions above 900 cm^{-1} and show only small differences in wave numbers for the bands with considerable intensity. More helpful for a distinction between the two isomers are the vibrational modes of the C_2PF_4 skeleton below 900 cm^{-1} . A significant evidence for the *trans* isomer is the appearance of the intense $\nu_{\text{as}}(\text{PC})$ at 823 cm^{-1} in the infrared and the intense $\nu_{\text{s}}(\text{PC})$ at 644 cm^{-1} in the Raman spectrum. The vibrational modes of the square planar PF_4 unit of *trans*- $[\text{Me}_2\text{PF}_4]^-$ are compared with *trans*- $[\text{MePF}_4\text{H}]^-$ and *trans*- $[\text{H}_2\text{PF}_4]^-$ in Table 4.^{17,23} The frequencies of the $\nu_{\text{s}}(\text{PF})$ modes decrease with the number of the methyl groups in the anion, whereas the frequencies of the $\nu_{\text{as}}(\text{PF})$ mode tend to increase. For the $\nu_{\text{as}}(\text{PF})$ as well as for the $\delta(\text{PF}_4)$ umbrella mode, smaller values should be expected for the $[\text{H}_2\text{PF}_4]^-$ anion. Christe et al. explained the different behavior by the influence of the light hydrogen ligands, since, for similar molecules with heavier axial ligands, the vibration was observed at lower wave numbers. Overall, the experimental frequencies of the

(23) Christe, K. O.; Schack, C. J.; Curtis, E. C. *Inorg. Chem.* **1976**, *15*, 135.

Table 3. Calculated (RHF/6-31+G*) Frequencies (cm⁻¹) of *Cis*- and *Trans*-Dimethyltetrafluorophosphate^a

<i>trans</i> -[Me ₂ PF ₄] ⁻				<i>cis</i> -[Me ₂ PF ₄] ⁻			
	IR-int.	Raman-act.	assignment		IR-int.	Raman-act.	assignment
2986.6	99.7	68.3	ν_{as} (CH ₃) in phase	2977.1	28.7	163.4	ν_{as} (CH ₃)
2986.1	8.2	69.0	ν_{as} (CH ₃)	2976.9	91.5	23.9	ν_{as} (CH ₃)
2985.4	98.3	60.7	ν_{as} (CH ₃) in phase	2954.9	17.3	57.8	ν_{as} (CH ₃)
2984.1	1.9	83.8	ν_{as} (CH ₃)	2953.1	117.4	73.4	ν_{as} (CH ₃)
2924.3	0.0	259.8	ν_s (CH ₃) in phase	2906.1	56.9	239.1	ν_s (CH ₃) in phase
2923.4	78.5	0.3	ν_s (CH ₃)	2899.3	17.5	8.6	ν_s (CH ₃)
1478.4	2.4	4.9	δ_{as} (CH ₃) in phase	1480.9	0.6	9.4	δ_{as} (CH ₃)
1477.4	2.1	4.7	δ_{as} (CH ₃) in phase	1479.5	2.8	0.5	δ_{as} (CH ₃) in phase
1477.2	0.1	9.5	δ_{as} (CH ₃)	1472.1	0.2	10.1	δ_{as} (CH ₃)
1475.7	0.0	6.8	δ_{as} (CH ₃)	1470.4	0.6	4.5	δ_{as} (CH ₃)
1353.9	38.6	0.0	δ_s (CH ₃)	1342.8	30.1	11.5	δ_s (CH ₃) in phase
1353.5	0.3	8.0	δ_s (CH ₃) in phase	1338.0	19.2	1.5	δ_s (CH ₃)
970.7	84.8	0.0	ρ (CH ₃) in phase	966.1	77.8	2.7	ρ (CH ₃)
969.6	82.5	0.0	ρ (CH ₃) in phase	952.9	90.1	0.5	ρ (CH ₃) I
931.3	0.0	2.8	ρ (CH ₃)	912.0	148.9	0.5	ρ (CH ₃)
930.9	0.2	2.9	ρ (CH ₃)	890.4	0.1	1.1	ρ (CH ₃)
821.0	328.4	0.1	ν_{as} (PC)	755.2	390.5	9.9	ν_s (PC/PF _{ax} _{iq})
683.7	405.6	0.1	ν_{as} (PF)	735.9	240.0	4.6	ν_{as} (PC/PF _{ax} _{iq})
682.8	405.3	0.1	ν_{as} (PF)	714.1	364.0	1.2	ν_{as} (PF _{ax})
626.5	0.0	26.4	ν_s (PC)	629.4	8.5	19.9	ν (C ₂ PF ₄) in phase
518.2	120.0	0.0	δ (PF ₄) umbrella	503.9	18.4	0.4	δ (F _{ax} PF _{ax} /F _{ax} PF _{ax})
501.1	0.3	6.1	ν (PF) in phase	499.3	17.6	3.1	ν_s (PF _{ax})
478.1	0.2	2.0	ν (PF) out of phase	496.7	13.9	6.0	ν_{as} (PF _{ax} /PC)
414.3	4.1	0.0	δ (CPC/FPF)	465.4	39.7	0.2	δ (F _{ax} PF _{ax})
411.8	4.0	0.0	δ (CPC/FPF)	456.3	8.0	0.3	δ (F _{2ax} PF _{ax} _{iq})
386.9	0.0	0.5	δ (CPF) sciss	390.0	0.5	0.6	δ (CPC)
379.4	0.0	0.6	δ (PF ₄) in plane	380.5	0.5	0.8	δ (F _{ax} PF _{ax})
377.6	0.2	0.5	δ (CPF) sciss	349.9	0.4	0.2	δ (C ₂ PF _{ax})
291.7	0.0	0.0	δ (PF ₄) out of plane	284.5	0.5	0.0	δ (F _{ax} PF _{ax} /F _{ax} PF _{ax})
257.1	0.6	0.0	δ (CPC/FPF)	279.7	0.1	0.0	δ (F _{ax} PF _{ax} /CPF _{ax} _{iq})
239.9	0.7	0.1	δ (CPC/FPF)	245.3	0.0	0.3	δ (C ₂ PF _{2ax} _{iq}) out of plane
50.8	0.0	0.3	τ (CH ₃)	124.0	0.1	0.0	τ (CH ₃)
1.4	0.2	0.0	τ (CH ₃) in phase	69.6	0.0	0.0	τ (CH ₃)

^a Frequencies are scaled with an empirical factor 0.91; IR intensities in km/mol; and Raman activities in Å⁴/u.

Table 4. Comparison of Experimental PF₄ Skeleton Vibrations (cm⁻¹) of *Trans*-[MePF₄H]⁻, [H₂PF₄]⁻, and [Me₂PF₄]⁻

Cs ⁺ [Me ₂ PF ₄] ⁻		Cs ⁺ [MePF ₄ H] ^{-a}		Cs ⁺ [H ₂ PF ₄] ^{-b}		assignment
IR	Raman	Raman	IR	Raman		
748 vs		683 (11)	700 vs, br		ν_{as} (PF)	
544 ms		538 (8)	610 s		δ (PF ₄) umbrella	
520 ms	512 (13)	563 (19)		576 (10)	ν (PF) in phase	
478 m	476 (6)	484 (21)		496 (2.6)	ν (PF) out of phase	
	379.4 ^c	399 (7)		397 (1.6)	δ (PF ₄) in plane	
	291.7 ^c	362 (2)	355 m		δ (PF ₄) out of plane	

^a From ref 17. ^b From ref 23. ^c Calculated.

PF vibrational modes of *trans*-[Me₂PF₄]⁻ fit into the series of known compounds. However, somewhat larger discrepancies occur in the calculated values. This might be due to a coupling between the vibrational modes. Under these circumstances, the absence of the *cis*-[Me₂PF₄]⁻ cannot be excluded by comparison of the vibrational modes of the C₂PF₄ skeleton. Finally, we compared the Raman spectrum of the single crystal of *trans*-[Me₂PF₄]⁻ with a Raman spectrum of the powdered whole sample, and we found no significant differences in the spectra. Thus, in accordance with the NMR spectra and the crystal structure, which is discussed later, only the *trans* isomer is observed in solution and in the solid state.

Theoretical Calculations. The geometric parameters from quantum chemical calculations on the RHF/6-31+G* and B3LYP/6-31+G* level of theory for *cis*- and

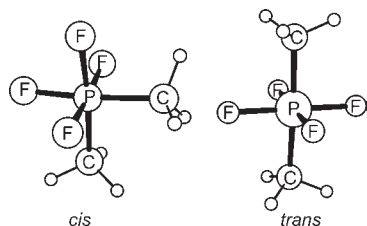
trans-dimethyltetrafluorophosphate are summarized in Table 5. Figure 2 shows the RHF-calculated structures of both isomers. Previous studies based on the comparison of experimental and calculated data have shown that RHF-calculations using the 6-31+G* base set satisfactorily reproduce the structures of phosphoranes and the corresponding fluoroanions.^{1,2,17,24} Calculations based on the B3LYP calculations using the same basis set tend to overestimate bond lengths, but because of the electron correlation, the energies calculated by this method are more accurate and used for further discussion.

The phosphorus atoms of the *trans*-[Me₂PF₄]⁻ and *cis*-[Me₂PF₄]⁻ anion both have an octahedral environment but significant differences in P–F and P–C bond lengths. The P–C distances of the *trans* species are shorter than that of the *cis* isomer at the expense of longer P–F bonds. Furthermore the F–P–F axis of the *cis* isomer has longer P–F bond lengths than the F–P–C axis. This is rather unexpected, since rationalizing the bonding situation in terms of semi-ionic three-center four-electron bonding, one would expect the opposite case due to a stronger semi-ionic contribution in the F–P–F axis.² The RHF-calculated trends for the bond length are also displayed by the B3LYP calculations, but all bond distances are longer and, in comparison with the crystal structure, overestimated. A comparison of the phosphoranes H₂PF₃,

(24) Kornath, A.; Neumann, F.; Ludwig, R. Z. Anorg. Allg. Chem. 2002, 628, 1835.

Table 5. Calculated Bond Distances (pm) and Angles (°) of *Cis*- And *Trans*-Dimethyltetrafluorophosphate

	<i>cis</i>		<i>trans</i>		expt
	RHF/6-31+G*	B3LYP/6-31+G*	RHF/6-31+G*	B3LYP/6-31+G*	
$r(\text{P}-\text{C})$	186.93	188.82	185.24	187.04	183.5
$r(\text{H}-\text{C})$	108.56	109.55	108.39	109.35	87.1–91.5
$r(\text{P}-\text{F})$	166.27	170.91			
$r(\text{P}-\text{F}')$	165.50	170.00	167.54	172.55	166.1–168.2
$\angle(\text{CPF})$	91.5	91.2			
$\angle(\text{CPF}')$	89.5	89.1	88.5, 91.4	88.6, 91.4	89.6–90.4
$\angle(\text{CPC})$	95.1	96.3	177.1	177.2	179.4
$\angle(\text{FPF})$	175.9	176.1	–	–	–
$\angle(\text{FPF}')$	88.5	88.6	–	–	–
$\angle(\text{F}'\text{PF}')$	85.9	85.6	89.2, 90.7	89.2, 90.8	89.7–90.3

**Figure 2.** Calculated (RHF/6-31+G*) structures of *cis*- and *trans*-dimethyltetrafluorophosphate.**Table 6.** Calculated (RHF/6-31+G*) Bond Lengths (pm) for Methyl- and Hydridophosphoranes and Hydridophosphates

	$[\text{MePF}_4\text{H}]^{-a}$	$[\text{H}_2\text{PF}_4]^{-a}$	$[\text{Me}_2\text{PF}_4]^{-}$	MePF_3H^b	H_2PF_3^a	Me_2PF_3^a
$r(\text{P}-\text{C})$	184.5	–	185.2	180.2	–	180.7
$r(\text{C}-\text{H})$	108.4	–	108.4	108.2	–	108.2
$r(\text{P}-\text{H})$	138.1	138.0	–	137.1	137.0	–
$r(\text{P}-\text{F})$	167.2	166.7	167.2	–	–	–
$r(\text{P}-\text{F}_{\text{ax}})$	–	–	–	163.4	162.3	164.7
$r(\text{P}-\text{F}_{\text{eq}})$	–	–	–	155.3	155.3	156.6

^a From ref 17. ^b From ref 24.

Me_2PF_3 , and MePF_3H and their corresponding phosphates formed by addition of a fluoride is given in Table 6. Insertion of a fluoride ion into a phosphorane changes the bonding situation dramatically. The axial P–F distances in the phosphoranes are elongated only by 4 pm, but the equatorial P–F distances are up to 12 pm longer in phosphates than in the phosphoranes. The increase of the equatorial bond distances shows the alteration from a mainly covalent P–F bond in the equatorial positions of the phosphoranes to semi-ionic three-center four-electron bonds in the phosphates.

The B3LYP-calculated difference of the Gibbs free energies between the two isomers is 29.4 kJ/mol^{−1}. This energy difference can be separated into enthalpic (24.0 kJ/mol) and entropic (5.4 kJ/mol) contributions. The entropic energy difference of both isomers is caused by the different torsion vibrations of the methyl groups, which is calculated for the *trans* and *cis* isomers at 1.6 and 69.9 cm^{−1}, respectively. Therefore, the *trans* isomer is entropically favored. This result is consistent with our previous studies on hydridomethyltetrafluorophosphate.¹⁷ For both anions, only the *trans* isomers are observed, and a transformation into a *cis* isomer is not possible at room temperature.

Crystal Structure of $\text{Me}_4\text{N}^+[\text{Me}_2\text{PF}_4]^-$. The crystal data are summarized in Table 7. The $\text{Me}_4\text{N}^+[\text{Me}_2\text{PF}_4]^-$ crystallizes in the orthorhombic space group *Pnma* with four formula units per unit cell. For the data reduction,

Table 7. Crystallographic Data of $\text{Me}_4\text{N}^+[\text{Me}_2\text{PF}_4]^-$

formula	$\text{C}_6\text{H}_{18}\text{NPF}_4$
formula weight, g mol ^{−1}	211.18
temperature °C	−116 (2)
space group	<i>Pnma</i> (no. 62)
<i>Z</i>	4
<i>a</i> , pm	1303.5(3)
<i>b</i> , pm	799.8(2)
<i>c</i> , pm	1023.8(2)
<i>V</i> , 10 ⁶ pm ³	1067.4(4)
density calcd, g cm ^{−3}	1.3142(5)
μ , abs coeff, cm ^{−1}	3.30
λ , pm	71.069
GOF an F^2	0.945
R^a [$I > 4\sigma(I)$]	$R1 = 0.0325$ $wR2 = 0.0797$
R^a (all data)	$R1 = 0.0784$ $wR2 = 0.2132$
largest diff peak and hole	0.331 and $-0.195 \text{ e} \cdot 10^6 \text{ pm}^3$

^a $R = \sum ||F_o| - |F_c|| / \sum |F_o|$; Refinement: full-matrix least-squares on F^2 .

Table 8. Selected Bond Distances (pm) and Angles (°) of $\text{Me}_4\text{N}^+[\text{Me}_2\text{PF}_4]^-$

P(1)–C(1)	183.4(3)	C(1)–P(1)–C(2)	179.4(1)
P(1)–C(2)	183.5(3)	C(1)–P(1)–F(1)	90.2(1)
P(1)–F(1)	166.9(1)	C(1)–P(1)–F(2)	89.8(1)
P(1)–F(2)	168.2(1)	F(1)–P(1)–F(2)	89.70(4)
P(1)–F(3)	166.1(1)	F(1)–P(1)–F(3)	90.30(4)
N(1)–C(3)	149.9(3)	F(2)–P(1)–F(3)	179.97(5)
N(1)–C(4)	149.7(3)	C(3)–N(1)–C(4)	109.2(2)
N(1)–C(5)	149.3(2)	C(3)–N(1)–C(5)	109.4(1)
F(1)···H(31)	241.8	C(4)–N(1)–C(5)	109.5(1)
F(1)···H(41)	241.8		
F(1)···H(51)	251.5		
F(2)···H(32)	250.7		
F(3)···H(32)	253.7		

structure solution, and refinement, SCALE PACK, programs in the SHELXTL package, and PARST were used.^{25–28} The phosphorus layers were found by the Patterson method. All atoms including hydrogen were found in the difference Fourier synthesis, and a final refinement with anisotropic (except for hydrogen atoms) thermal parameters gave an *R* value of 0.0325.²⁹

(25) Otwinowski, Z.; Minor, W. *Methods Enzymol.* **1997**, *276*, 307.

(26) Sheldrick, G. M. *SHELXTL PLUS an Integrated System for Solving, Refining, and Displaying Structures from Diffraction data*; University of Göttingen, Göttingen, Germany, 1987.

(27) Sheldrick, G. M. *SHELXL 93*; University Göttingen, Germany, 1993.

(28) Nardelli, M. *Comput. Chem.* **1993**, *7*, 95.

(29) More details about the crystal structure are available at the Fachinformationszentrum Karlsruhe, Gesellschaft für Wissenschaftlich-Technische Informationen mbH, D-76344 Eggenstein-Leopoldshafen, under the deposition number CSD-420584.

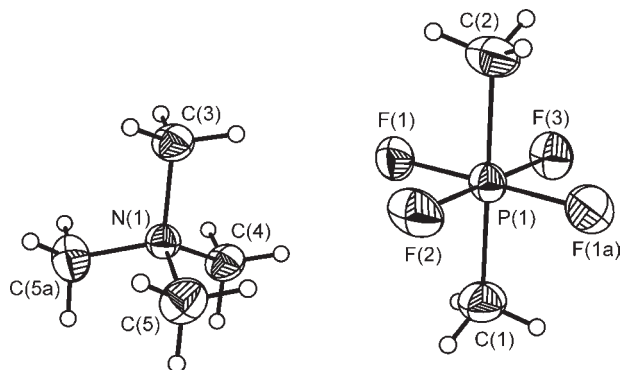


Figure 3. Asymmetric part of the unit cell of $\text{Me}_4\text{N}^+[\text{Me}_2\text{PF}_4]^-$. Thermal ellipsoids are drawn at 50% probability level. Symmetry transformation: (a) $x, 0.5 - y,$ and z .

Bond lengths and selected angles are summarized in Table 8. The asymmetric part of the unit cell is presented in Figure 3. The phosphorus atom of the anion has an octahedral environment with bond angles slightly deviating from 90 or 180°, respectively, and a *trans* arrangement of the methyl groups. The P–F distances between 166.1(1) and 168.2(1) pm are in the regular range for fluorophosphates. Overall, the geometry parameters of the anion are well reproduced by the RHF calculation. Only the

(30) Minkwitz, R.; Schneider, S.; Kornath, A. *Inorg. Chem.* **1998**, *37*, 4662.

(31) Kornath, A.; Blecher, O. *Z. Naturforsch.* **1999**, *54b*, 372.

(32) Kornath, A.; Blecher, O.; Ludwig, R. *Z. Anorg. Allg. Chem.* **2002**, *628*, 183.

(33) Bondi, A. *J. Phys. Chem.* **1964**, *68*, 441.

calculated P–C bond is 1.7 pm longer than its experimental value.

For the cation, the lengths of the N–C bonds and the C–N–C angles show only small deviations from the ideal tetrahedral geometry and are in good agreement with known Me_4N^+ salts.^{30–32} Weak interactions are observed between eight hydrogen atoms of one cation and all fluorine atoms of the anions ranging from 241.8 to 253.7 pm (sum of the van der Waals radii is 267 pm).³³ Cations and anions are stacked alternating along the crystallographic *b*-axis and are linked together via the weak $\text{H}\cdots\text{F}$ interactions forming a three-dimensional network.

Conclusion

The $[\text{Me}_2\text{PF}_4]^-$ anion, previously observed in solutions only, was prepared and isolated as salt of Na, K, Cs, Me_4N , and Me_4P . These results demonstrate that the Lewis acidity of Me_2PF_3 is higher than previously assumed. NMR, infrared, and Raman spectra as well as a single crystal structure show the exclusive formation of the *trans* isomer in solutions and in the solid state. This is in accordance with theoretical calculations which yielded a difference of the Gibbs free energy of 29.4 kJ/mol (B3LPY/6-31+G*) between the *cis* and *trans* isomer.

Acknowledgment. This work was supported by the Deutsche Forschungsgemeinschaft.

Supporting Information Available: The crystallographic data in CIF format. This material is available free of charge via the Internet at <http://pubs.acs.org>.